JOURNAL OF CATALYSIS 127, 465–488 (1991)

CO Oxidation over Pd and Cu Catalysts

I. Unreduced $PdCl_2$ and $CuCl_2$ Dispersed on Alumina or Carbon

KYUNG I. CHOI AND M. ALBERT VANNICE

Department of Chemical Engineering, The Pennsylvania State University, University Park, Pennsylvania 16802

Received May 9, 1990; revised August 27, 1990

CO can be oxidized at 300–400 K by molecular oxygen over dispersed, unreduced $PdCl_2$ or $CuCl_2$ although rates were much lower than those obtained using both compounds together. $PdCl_2$ was much more active than $CuCl_2$, and the addition of water vapor to the feed greatly enhanced the activity of the $PdCl_2$ catalysts but not the $CuCl_2$ catalysts. This system had not been previously characterized by IR spectroscopy, so this technique was employed to determine the Pd and Cu carbonyl and chloro-carbonyl species formed upon the introduction first of CO then, sequentially, of H_2O and O_2 to establish reaction conditions. The *in situ* spectra identified $PdCl_2CO$, $(PdClCO)_n$, and CuClCO species as well as a small amount of terminal and bridged CO adsorbed on metallic Pd particles. Based upon the IR results, a thorough kinetic study, and prior aqueous-phase studies in the literature, a reaction model is proposed that involves water as a reactant with the PdClCO species when water vapor is present. In its absence, molecular oxygen appears to interact with PdClCO to produce CO_2. © 1991 Academic Press, Inc.

INTRODUCTION

The catalytic oxidation of carbon monoxide provides one route to remove this pollutant from automotive exhausts as well as from factory effluent gas streams. In addition, the catalytic removal of carbon monoxide at room temperature has practical importance because of its use in the purification of indoor air (*1*) and in CO leak detection. One oxide catalyst—hopcalite, which is a mixture of MnO_2, CuO, and several other oxides—is currently used for the latter application; however, its major disadvantage is its deactivation in the presence of moisture, and this severely limits its practical use (*2*). This reaction over Group VIII metal catalysts was first investigated by Langmuir in 1922 (*3*), and CO oxidation has been frequently studied over both single-crystal Pd surfaces and well-dispersed, supported Pd crystallites (*4–13*). This reduced metal typically provides substantial activity at temperatures above 373 K, which is a general characteristic of the Group VIII metals. CO oxidation over copper oxide has also been investigated, and a higher reaction temperature is needed to obtain the same degree of activity (*14–16*).

An alternative approach to achieve high activity at low temperature is the use of a homogeneous, rather than a heterogeneous, catalyst. Aqueous solutions of $PdCl_2$–$CuCl_2$ are commercially used in the Wacker process to produce acetaldehyde from ethylene and dioxygen at low temperature, and this system was found to also catalyze CO oxidation at room temperature (*17–18*). The activity could be enhanced by dispersing this solution on an oxide support (*17*), and Desai *et al.* found that Al_2O_3 impregnated with an unreduced solution of $PdCl_2$ and $CuCl_2$ was very active at low temperature provided the humidity was neither too high nor too low (*19–20*). CO oxidation catalyzed by aqueous solutions of Pd(II) has been extensively studied by several groups of Russian investigators. It has been proposed by Golodov *et*

0021-9517/91 $3.00
Copyright © 1991 by Academic Press, Inc.
All rights of reproduction in any form reserved.

al. that water, rather than O_2, is the oxidant although oxygen can enhance activity (*21*), while Zhizhina and co-workers have proposed that Pd(I) carbonyl complexes are the catalytically active species and these complexes interact with O_2 (*22, 23*). However, CO oxidation by O_2 in $PdCl_2$-only systems has had little attention and only one kinetic study has been reported (*24*). Also, as stated by Kuznetsova *et al.*, insufficient work has been done to allow one to be specific about the active intermediate species formed in the presence of H_2O or O_2 (*25*). Similarly, CO oxidation over unreduced Cu compounds has not been examined although the water gas shift reaction has been studied (*26*).

This study was therefore conducted to: (1) determine the kinetic behavior of CO oxidation over unreduced $PdCl_2/Al_2O_3$, $CuCl_2/Al_2O_3$, and bimetallic $PdCl_2$–$CuCl_2/Al_2O_3$ catalysts, (2) use *in situ* IR spectroscopy before and during reaction conditions to identify the Pd species present, (3) see if a reaction sequence consistent with both the kinetic and the IR data could be proposed, and, finally, (4) utilize the insight gained to improve the performance of this system by employing an appropriate carbon support to control water adsorption. This paper describes the single-metal catalysts on alumina and carbon while the second paper discusses the unreduced, bimetallic Pd Cl_2–$CuCl_2$ catalysts (*27*). The behavior of these three catalyst systems after reduction in hydrogen is discussed in the final part of this series (*28*).

EXPERIMENTAL

Supported Pd and Cu catalysts were made by an incipient wetness method (*29*). The supports were δ-Al_2O_3 (W. R. Grace, 138 m^2/g) and carbon black (Black Pearls 2000, Cabot Corp., 1400 m^2/g). The metal precursors were $PdCl_2$ (Alfa Products) and $CuCl_2$ (99.999%, Aldrich Chemical Co.). Before preparing these catalysts, the δ-Al_2O_3 was ground and sieved to a 40/80 mesh size and calcined in dry air (825 cc/min) at 723 K for 2.5 h. The carbon was evacuated at 723 K overnight to remove any adsorbed water. Catalyst preparation was based upon established methods (*29–31*), using distilled, deionized (DD) water and the appropriate amount of metal salt dissolved in 1.15 cm^3 solution per g Al_2O_3 and 2.04 cm^3 solution per g carbon. The prepared catalysts were then equilibrated overnight in the open atmosphere at 300 K and stored.

Product analyses from either the IR reactor cell or the stainless steel microreactor were obtained with a Perkin–Elmer Sigma 3 gas chromatograph using a Porapak column for peak resolution and a Perkin–Elmer Sigma 1 integrator for peak analysis. Flows of CO, O_2, and He were controlled by micrometer values and monitored by Hastings–Raydist mass flowmeters. When present, the water vapor pressure was controlled with a constant temperature bath by bubbling the feed gases through a sparger into the DD-water held in a 100-cm^3 flask which was immersed in a 70% water/30% isopropanol bath. The saturator contained a bypass arrangement to permit either wet or dry CO/O_2 mixtures to be fed into the reactor. For kinetic studies *ex situ* of the IR reactor cell, a separate $\frac{1}{4}''$ stainless steel reactor containing 0.1–0.2 g catalyst and a temperature-controlled furnace were used.

For simultaneous *in situ* kinetic/IR spectroscopic studies, specially designed cylindrical, stainless steel reactors with NaCl windows were used into which thin wafers were pressed. The faces of the stainless steel pistons, used to press the powder, were ground and polished with very fine polishing material (600 aluminum powder) and the edge of the bottom piston was beveled. A copper wire with the same volume as the beveled space was pressed into that volume with 6000 psig using a Carver press. This produced a copper ring adhering to the wall of the stainless steel reactor which supported the wafer then pressed into the cylinder. The catalyst was finely ground with an agate mortar and dried in the oven at 393 K for 1.3 h before it was pressed. About 40 mg

of catalyst powder was evenly distributed on the piston surfaces, and it was then pressed at 5000 psig for 20 min. Wax paper was inserted between the catalyst and the pistons to prevent the catalyst from sticking to the piston faces. The thickness of the pressed wafer was about 0.15 mm. All the feed gas passed through this wafer, which acted as a small, fixed-bed differential reactor, and into the GC sampling valve. Bed temperatures up to 648 K could be attained. The IR spectrometer was a Perkin–Elmer 580 which had been coupled to an Apple II computer and color monitor via an A/D converter to allow further analysis of the IR spectra when desired. Further details and a diagram of this system have been provided previously (*32*).

The procedure for the simultaneous *in situ* kinetic/IR spectroscopic runs was as follows: a background spectrum under He was acquired before the spectrum at 303 K under 26.3 Torr CO (unless otherwise noted) in flowing He was obtained. Then spectra were acquired with this gas mixture saturated with H_2O at 275 K (5.3 Torr H_2O), and finally O_2 was added at 132 Torr partial pressure and additional spectra were obtained. Studies in the absence of water were conducted in a similar sequence, but the H_2O addition was omitted. During each IR spectrum, the composition of the outlet gas from the reactor was analyzed by the GC, and all IR peaks were stored in the Apple computer connected to the IR spectrometer. After obtaining these spectra, Arrhenius and partial pressure dependency runs were conducted. Finally, if needed, additional experiments were then performed. Essentially only Arrhenius and partial pressure dependency runs were conducted with the microreactor outside the IR spectrometer. Standard reaction conditions consisted of flowing gas at 100 kPa (1 atm), 132 Torr O_2 (17.4 kPa), 26 Torr CO (3.4 kPa) with the balance composed of He. The reaction orders with respect to CO were determined at 132 Torr O_2 while the reaction orders with respect to O_2 were determined at 26 Torr CO.

RESULTS

The kinetic behavior of supported, unreduced $PdCl_2$ or $CuCl_2$ catalysts in the presence and absence of H_2O vapor is given in Tables 1 and 2, and typical Arrhenius plots for these catalysts are shown in Figs. 1 and 2. During the initial Arrhenius run, erratic behavior was sometimes observed, as in Figs. 1a and 1d, for example, and this was associated with removal of water from the catalyst. No activation energies in Table 1 were determined from these data. Specific activities in the form of a nominal turnover frequency (TOF) are also included, and they are computed with the assumption that the dispersion of the $PdCl_2$ or $CuCl_2$ precursor is unity, thus they represent the lowest possible values. Partial pressure dependencies were determined and initially fitted by a power rate law over certain pressure regimes, which were from 0.5 to 184 Torr for CO, from 26 to 184 Torr for O_2, and from 2 to 20 Torr for H_2O, and they are shown in Fig. 3.

Over the 2% Pd/δ-Al_2O_3 catalyst at 403 K with no water vapor, the partial pressure dependency on CO was negative (-0.4), which is similar to previous trends for the noble metals (*33*), while that for O_2 was positive (0.6) when $P_{CO} > P_{O_2}$, but was near zero when $P_{CO} < P_{O_2}$, as shown in Table 2 and Fig. 3a. The activation energy was 16.5 kcal/mole from the IR reactor results and 18.1 kcal/mole from the kinetic study in the microreactor, as shown in Table 1. Sometimes the first run exhibited a significant change in activity after the temperature cycle was completed, and this was attributed to a change in the amount of adsorbed water.

The 12% Cu/δ-Al_2O_3 catalyst at 423 K with no water vapor gave a positive partial pressure dependency on CO (0.5), which again is consistent with earlier studies of Group IB metals (*34*), and that of O_2 was slightly positive (0.2), as shown in Fig. 3b. The activation energy for this catalyst was 21.6 kcal/mole from the IR reactor study and 16.6 kcal/mole from the kinetic study in

TABLE 1

Catalytic Activities and Apparent Activation Energies for CO Oxidation over Unreduced $PdCl_2$ and $CuCl_2$ Catalysts

Catalyst	P_{H_2O} (Torr)	E_{app}[a] (k/cal/mole)	Activity[b] at 300 K (μmole CO/g cat · s × 10^3	TOF[b,c] at 300 K (s^{-1})
2% Pd/δ-Al_2O_3	0	16.5 ± 0.4[d]	0.08	4×10^{-7}
(IR)	5.3	11.5 ± 1.8	27.4	1.5×10^{-4}
2% Pd/δ-Al_2O_3	0	18.1 ± 0.2[e]	0.02	1.0×10^{-7}
(reactor) Run 1	5.3	9.2 ± 0.03	2.7	1.4×10^{-5}
Run 2		8.6 ± 0.05		
2% Pd/carbon	5.3	4.7 ± 0.1	16.9	1.0×10^{-4}
(reactor) Run 2				
12% Cu/δ-Al_2O_3	0	21.6 ± 0.2[f]	0.09	5×10^{-8}
(reactor) Run 2				
12% Cu/δ-Al_2O_3	0	16.6 ± 1.8	0.01	5×10^{-9}
(IR) Run 2				
12.08% Cu/carbon	5.3	12.3 ± 0.06	0.2	1×10^{-7}
(reactor)				

[a] With 95% confidence limits.
[b] Standard reaction conditions: P_{O_2} = 132 Torr, P_{CO} = 26 Torr, total p = 750 Torr.
[c] TOF = molecule CO reacted per second per metal atom.
[d] Descending T, from Fig. 1a.
[f] Run 2 from Fig. 1d.

TABLE 2

Partial Pressure Dependencies on CO, O_2, and H_2O for CO Oxidation over Unreduced $PdCl_2$ and $CuCl_2$ Catalysts

Catalyst	Partial pressure dependency[a]			Partial pressure run temp. (K)
	X	Y	Z	
2% Pd/δ-Al_2O_3	−0.4	0.6($P_{O_2} > P_{CO}$)	No H_2O	403
(IR)	−0.7	1.2	0.7	
2% Pd/δ-Al_2O_3	−0.2	0.9	No H_2O	343
(reactor)	−0.2	1.0	No H_2O	363
	−0.2	0.8	No H_2O	383
2% Pd/carbon	0.1	0.5	0.6	353
(reactor)				
12% Cu/δ-Al_2O_3	0.5	0.2	No H_2O	423
(reactor)				
12.8% Cu/carbon	0.7	0.5	−0.3	433
(reactor)				

[a] $r = k P_{CO}^X P_{O_2}^Y P_{H_2O}^Z$. P_{CO} = 26 Torr when Y and Z were obtained; P_{O_2} = 132 Torr when X and Z were obtained; P_{H_2O} = 5.3 Torr when X and Y were obtained.

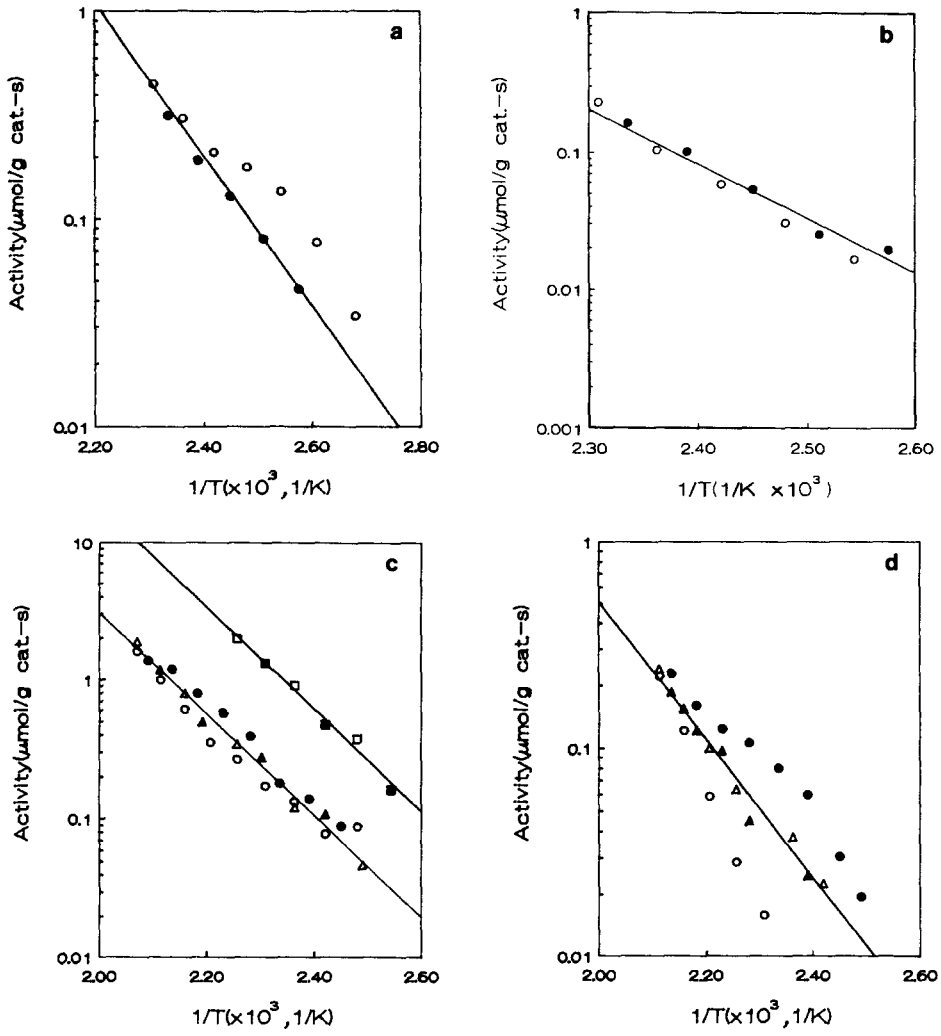

FIG. 1. Arrhenius plots for uncalcined and unreduced $PdCl_2$ and $CuCl_2$ catalysts in the absence of water vapor in the feed. Total pressure = 750 Torr, P_{CO} = 26 Torr, P_{O_2} = 132 Torr, balance was He; Run 1—circles; Run 2—triangles; Run 3 (after O_2 treatment)—squares; open symbols, ascending temp.; closed symbols, descending temp.

(a) 2% Pd/δ-Al_2O_3 (IR);
(b) 2% Pd–δ-Al_2O_3 (reactor);
(c) 12% Cu/δ-Al_2O_3 (IR);
(d) 12% Cu/δ-Al_2O_3 (reactor).

the microreactor. After a treatment at 573 K for 1 h in O_2 (13 Torr), the activity was enhanced but the activation energy was unchanged, as shown in Fig. 1c.

In the presence of 5.3 Torr H_2O, the activities were markedly higher, and the 2% Pd/δ-Al_2O_3 catalyst at 323 K again had a negative partial pressure dependency on CO (−0.7 from the IR study and −0.2 from the microreactor study), and a stronger, first-order dependency on O_2 was obtained. The H_2O partial pressure dependency was 0.7.

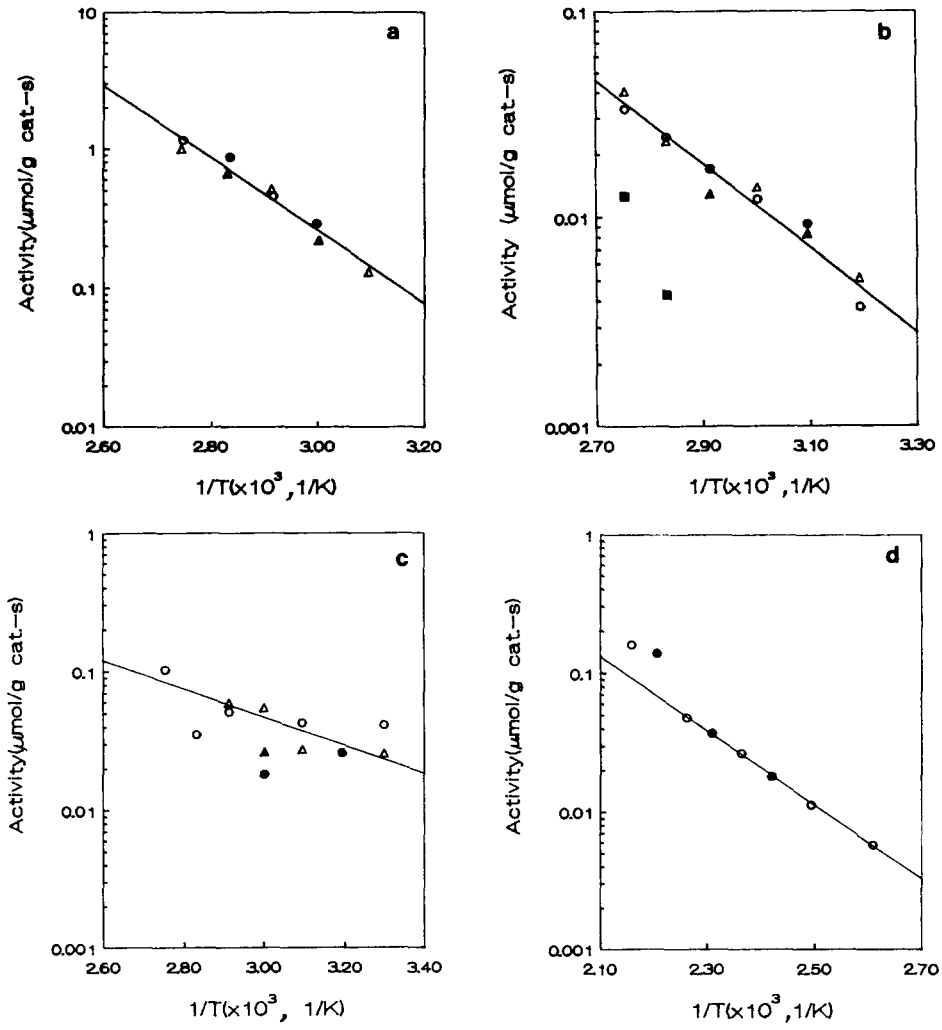

FIG. 2. Arrhenius plots for uncalcined and unreduced $PdCl_2$ and $CuCl_2$ catalysts with water vapor in the feed. Total pressure = 750 Torr, P_{CO} = 26 Torr, P_{O_2} = 132 Torr, P_{H_2O} = 5.3 Torr, balance was He; Run 1—circles; Run 2—triangles; Run 3 (without water vapor)—squares; open symbols, ascending temp.; closed symbols, descending temp.

(a) 2% Pd/δ-Al_2O_3 (IR);
(b) 2% Pd/δ-Al_2O_3 (reactor);
(c) 2% Pd/carbon (reactor);
(d) 12% Cu/carbon (reactor).

The activation energy for this catalyst was somewhat lower in the presence of water (9–13 kcal/mole). With the 12% Cu/δ-Al_2O_3 catalyst in the presence of water vapor, no detectable activity was obtained until temperatures were above 353 K. As the reaction orders on CO and O_2 for Pd/δ-Al_2O_3 were acquired at much lower temperatures, no partial pressure runs were conducted for this Cu/δ-Al_2O_3 catalyst.

Because of the black-body behavior of the carbon support, no dispersive IR spectra could be obtained, consequently all studies were conducted in the microreactor. For the

2.11% Pd/carbon catalyst at 353 K in the presence of 5.3 Torr H_2O, the partial pressure dependencies on CO and O_2 were 0.1 and 0.5, respectively, while the H_2O partial pressure dependency was 0.6. The activation energy for this catalyst was very low, i.e., 4.7 kcal/mole, which could imply mass transfer limitations, and the activity was six times greater than the comparable Pd/Al_2O_3 catalyst. This improved performance indicates an important advantage for the use of carbon supports and implies that the extent of adsorbed H_2O plays an important role in CO oxidation. The 12.08% Cu/carbon catalyst was again quite inactive, and the temperature had to be raised to 433 K to obtain detectable activity. The partial pressure dependencies on CO, O_2, and H_2O were 0.7, 0.5, and -0.3, respectively, and the activation energy was 12.3 kcal/mole. Direct comparison of these results with those from the $PdCl_2$ catalysts is somewhat difficult because of the significant difference in temperature. Also, there was a jump in activity around 453 K, as shown in Fig. 2d, whose cause is not precisely known but may possibly be due to removal of CO_2 produced from the decomposition of functional groups on the carbon surface (*35*).

With the 2% Pd/δ-Al_2O_3 wafer, an IR spectrum at a low CO pressure of 0.4 Torr was obtained (Fig. 4b) before the pressure was increased to 26 Torr CO in He. At 303 K under either pressure, CO peaks at 1930, 1990, 2090, 2100, and 2158 cm^{-1} were obtained, as shown in Figs. 4b and 4c. The 1930-cm^{-1} peak was the strongest, while the 2090- and 2100-cm^{-1} bands overlapped. Under reaction conditions with 132 Torr of O_2 present, peak positions and peak intensities were essentially unchanged, as shown in Fig. 4d. During the first cycle to measure activation energies, the peak shapes changed gradually and their intensities decreased, as shown in Fig. 4e. Finally, at 423 K the 1930-cm^{-1} peak, which initially was sharp and symmetric, became broadened and much less intense while the 2105- and 2158-cm^{-1} peaks disappeared (Fig. 4f). After cooling and returning to the original reaction conditions, the broad 1930-cm^{-1} band was retained and a weaker, broader 2090-cm^{-1} band grew back. Only these latter bands were observed in subsequent kinetic runs, and the original bands were not reattained.

On another 2% Pd/δ-Al_2O_3 wafer, 26.3-Torr CO balanced with He was fed to the reactor and the subsequent IR spectrum had peaks at 1930, 1990, 2090, and 2100 cm^{-1}, as shown in Fig. 5b. Again, the 1930-cm^{-1} band was the strongest, and the 2090 and 2100-cm^{-1} peaks overlapped. With the addition of 5.3 Torr H_2O in the feed, the 1930-cm^{-1} peak was greatly suppressed and the 2100-cm^{-1} peak disappeared (Fig. 5b).

Under reaction conditions with 132 Torr of O_2 added to the feed, the 1930-cm^{-1} peak was further suppressed only to a small extent, as shown in Fig. 4d, and little change occurred in the other bands. Again the 1930-cm^{-1} peak never recovered its initial intensity; however, at higher reaction temperatures (at 353 K and 363 K) the 1930-cm^{-1} peak intensity increased somewhat, but it reversibly returned to its lower intensity when the temperature was decreased back to 323 K.

Finally, with a 12% Cu/δ-Al_2O_3 wafer, only one peak at 2115 cm^{-1} was obtained under CO in He, and its intensity and position were essentially unchanged upon the addition first of H_2O, then also of O_2, as shown in Fig. 6.

DISCUSSION

Infrared Spectra

Although palladium has been extensively used as a homogeneous catalyst for the synthesis of aldehydes and ketones from olefins (*36*), the chemistry of halo-carbonyl complexes of palladium is still far from being completely understood. One major reason for this is the extremely unstable nature of these halo-carbonyl complexes of palladium in air or around moisture (*37*). Manchot and Konig first reported a compound with the

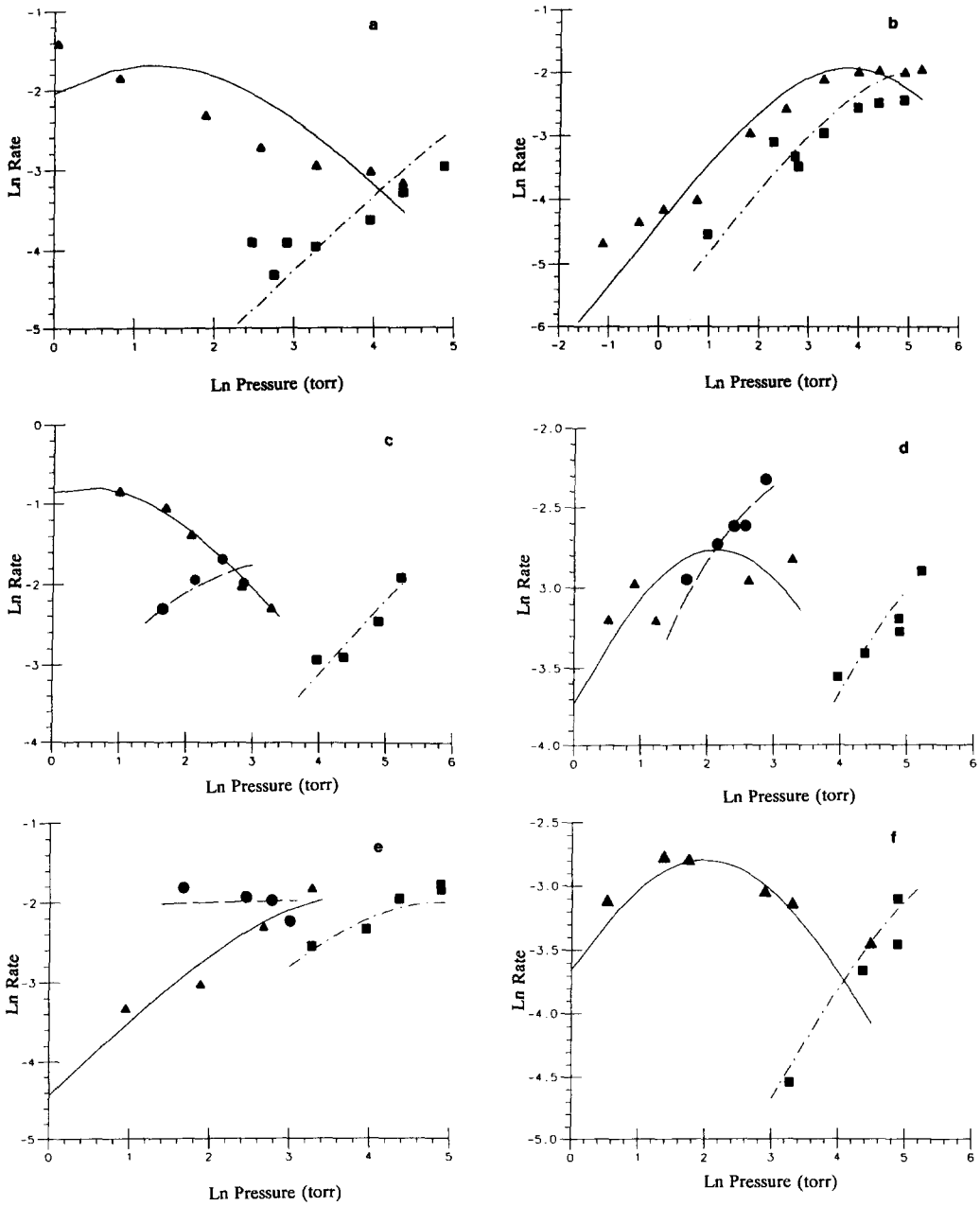

FIG. 3. Comparison between data and rates (μmole/g cat · s) predicted from the model for CO oxidation over supported $PdCl_2$ and $CuCl_2$ catalysts: CO (▲), O_2 (■), H_2O (●).

(a) 2% Pd/δ-Al_2O_3 at 403 K without water vapor (IR), Eq. (29);

(b) 12% Cu/δ-Al_2O_3 at 423 K without water vapor (IR), Eq. (29);

(c) 2% Pd/δ-Al_2O_3 at 323 K with water vapor (IR), Eq. (32);

(d) 2% Pd/carbon at 353 K with water vapor (reactor), Eq. (32);

(e) 12% Cu/carbon at 433 K with water vapor (reactor), Eq. (32);

(f) 2% Pd/δ-Al_2O_3 at 363 K with water vapor (reactor), Eq. (32);

(g) CO dependencies over 2% Pd/δ-Al_2O_3 at 383 K with water vapor before (▲) and after (●) O_2 treatment (reactor), Eq. (32);

(h) O_2 dependencies over 2% Pd/δ-Al_2O_3 at 383 K with water vapor before (■) and after (▼) O_2 treatment (reactor), Eq. (32).

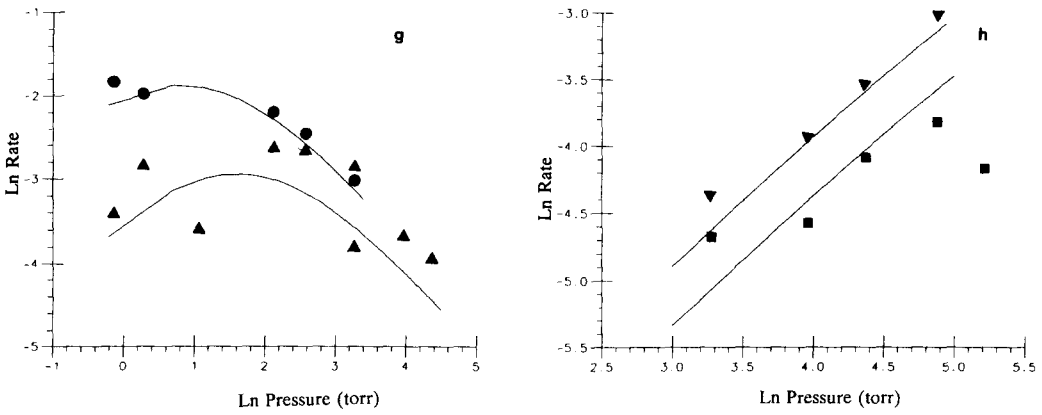

FIG. 3—*Continued*

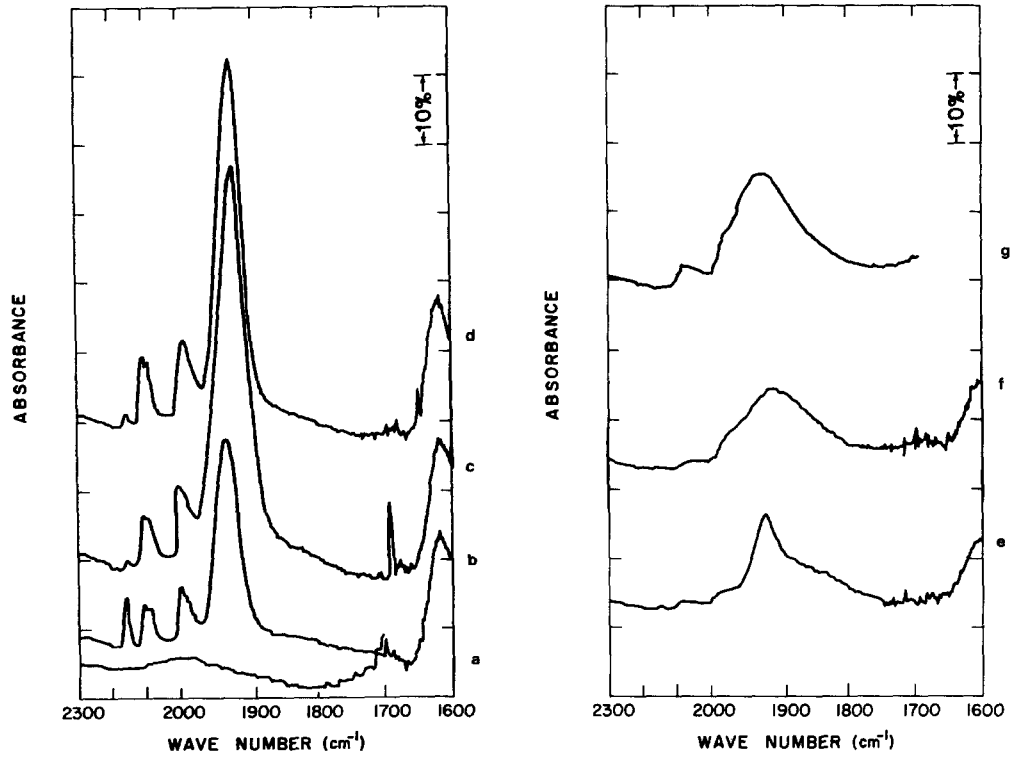

FIG. 4. Sequential IR spectra for 2% Pd/δ-Al_2O_3 in the absence of water vapor in the feed. Gas flow = 28.5 cm^3/min, Total pressure = 750 Torr.

(a) He only at 303 K;
(b) He + 0.4 Torr CO at 303 K;
(c) He + 26 Torr CO at 303 K;
(d) He + 26 Torr CO + 132 Torr O_2 at 303 K;
(e) He + 26 Torr CO + 132 Torr O_2 at 393 K;
(f) He + 26 Torr CO + 132 Torr O_2 at 423 K;
(g) He + 26 Torr CO + 132 Torr O_2 at 303 K (final).

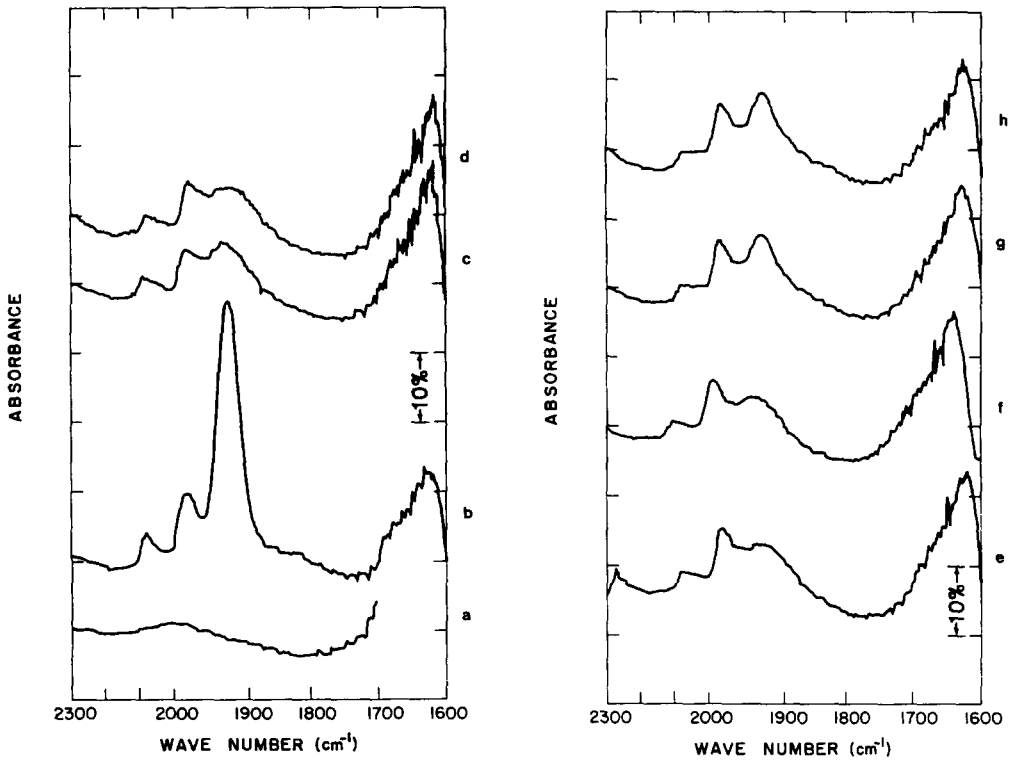

FIG. 5. Sequential IR spectra for 2% Pd/δ-Al_2O_3 with water vapor in the feed. Gas flow = 28.5 cm^3/min, total pressure = 750 Torr.

(a) He only at 303 K;
(b) He + 26 Torr CO + 303 K;
(c) He + 26 Torr CO + 5.3 Torr H_2O at 303 K;
(d) He + 26 Torr CO + 5.3 Torr H_2O + 132 Torr O_2 at 303 K;
(e) He + 26 Torr CO + 5.3 Torr H_2O + 132 Torr O_2 at 343 K;
(f) He + 26 Torr CO + 5.3 Torr H_2O + 132 Torr O_2 at 363 K;
(g) He + 26 Torr CO + 5.3 Torr H_2O + 132 Torr O_2 at 353 K;
(h) He + 26 Torr CO + 5.3 Torr H_2O + 132 Torr O_2 at 323 K.

composition $PdCOCl_2$ (*38*), but it was not until 1958 that Irving and Magnusson reported IR spectra showing a carbonyl absorption band at 1976 cm^{-1} for a compound with this elemental analysis (*39*). A strong absorption peak at 1947 cm^{-1} was reported by Sanger *et al.* (*40*) for $PdCOCl_2(PhCN)$, and Andronov *et al.* (*41*) showed that CO absorption in compounds of the type [Pd(CO)LCl_2], where L is a sulfur-containing ligand, lies between 1900 and 2000 cm^{-1}. Spitsyn *et al.* (*42*) showed that the IR spectrum of Cs[Pd(CO)Cl_3] in liquid paraffin has a characteristic wavenumber at 1930 cm^{-1} and found that this compound is extremely sensitive to moisture and decomposes rapidly in air to give a black product.

All these reports have mentioned CO frequencies between 1900 and 2000 cm^{-1}, which are too low for terminal carbonyl groups of late transition elements. Goggin *et al.* (*43*) reported that the dimeric d^9 Pd(I) anion $[Pd_2(CO)_2Cl_4]^{-2}$ exists in both solid state and solution, as shown by X-ray structure analysis and IR spectroscopy. In CH_2Cl_2, IR spectra showed a carbonyl stretching frequency at 1966 cm^{-1} of medium intensity, assigned to symmetric

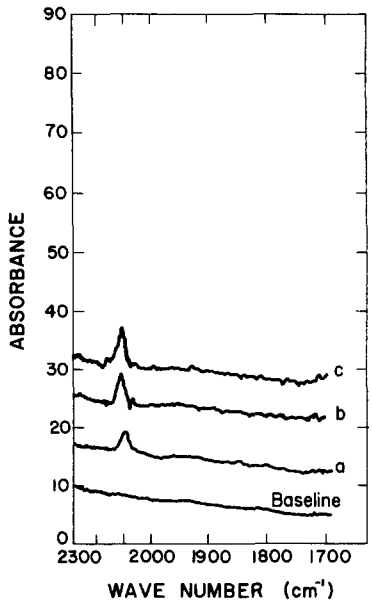

FIG. 6. Sequential IR spectra for 12% $Cu/\delta\text{-}Al_2O_3$ with and without water vapor. Gas flow = 28.5 cm^3/min, Total pressure = 750 Torr.
(a) He + 26 Torr CO at 303 K;
(b) He + 26 Torr CO + 5.3 Torr H_2O at 303 K;
(c) He + 26 Torr CO + 5.3 Torr H_2O + 132 Torr O_2 at 303 K.

stretching, and a strong band at 1906 cm^{-1}, assigned to asymmetric stretching. Goggin and Mink (*44*) reported that the $(PdCOCl)_n$ species has a very strong, broad CO stretching frequency at 1978 cm^{-1}, assigned to an asymmetric stretch, and several very weak peaks at 2023, 2002, 1951, and 1936 cm^{-1}. This Pd carbonyl complex has been proposed to exist in a chain structure, as shown in Fig. 7.

They also reported that the $Pd(CO)_3$ ClPhCN species has strong peaks at 1954 and 1948 cm^{-1}, assigned to the asymmetric stretches near the end of the chain which are *trans* to Cl and PhCN, and a medium intensity peak at 1979 cm^{-1}, assigned to a central asymmetric stretch, as in $(PdCOCl)_n$. The proposed structure of this latter species is depicted in Fig. 8. Other IR studies (*37, 45–48*) have been conducted with $[PdCOCl]_n$ complexes and have found that the stretching frequencies of CO lie between 1900 and 2000 cm^{-1}.

IR frequencies for the terminal carbonyl groups in Pd(II) compounds have been determined in several studies (*44, 50, 51*). Calderazzo and Dell'Amico (*50*) measured CO frequencies for $[PdCOCl_3]^{-1}$ at 2146 cm^{-1} in CH_2Cl_2 solution and 2141 cm^{-1} in Nujol, respectively, while Browning *et al.* (*51*) reported CO frequencies for $[PdCOCl_3]^{-1}$ at 2132 cm^{-1} in CH_2Cl_2 solution and 2120 cm^{-1} in a mull. Calderazzo and Dell'Amico (*50*) also showed that the carbonyl stretching frequencies in the $[Pd_2(CO)_2Cl_4]$ complex, assumed to be the dimeric *trans* structure in Fig. 9, lie in the range of 2159–2167 cm^{-1} in several solvents. Based on these later studies, it appears that the earlier assumptions that the terminal CO ligands gave bands between 1900 and 2000 cm^{-1} are incorrect, and the authors were most likely measuring spectra associated with dimers or polymers provided by bridge-bonded CO.

Frequencies of CO adsorbed on palladium metal surfaces have been reported in numerous studies, which have been reviewed elsewhere (*52–54*). Basically, they lie in three regions: 2050–2120 cm^{-1}, associated with singly bonded (terminal) CO; 1800–2000 cm^{-1}, associated with doubly bonded (bridged) CO; and 1800–1880 cm^{-1}, associated with triply bonded CO (*53*). Kundig *et al.*(*55*) reported the frequency of CO in $Pd(CO)_4$ to be 2060 cm^{-1} and proposed the structure in Fig. 10. Several investigations have shown that the vibrational frequencies of bridge-bonded CO attached to zero-valent Pd clusters are typically below 1890 cm^{-1} (*56–60*), thus these values are lower

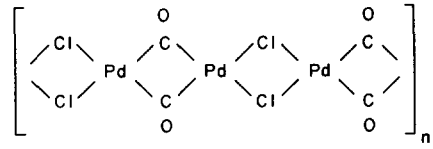

FIG. 7. The structure of $(PdCOCl)_n$ proposed by Goggin and Mink (*44*).

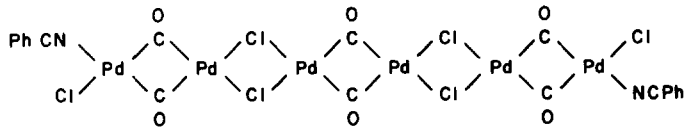

FIG. 8. The structure of $Pd(CO)_3ClPhCN$ proposed by Gogin and Mink (*44*).

than similarly coordinated CO on Pd crystal surfaces. An especially low value of 1720 cm^{-1} was obtained for CO coordinated through a particularly wide Pd–C–Pd angle (*60*).

Vargaftik *et al.*(*61*) surveyed the carbonyl complexes of palladium in oxidation states of (0), (I), and (II), and they concluded that the values of carbonyl frequencies within the fairly narrow range of 2140–2163 cm^{-1} correspond to terminal CO and depend little on the nature of the other ligands. They also concluded that the carbonyl chloride with the stoichiometry of $PdCOCl_2$, whose frequency was reported by Irving and Magnusson to be 1976 cm^{-1} (*39*), exists as a polynuclear compound containing bridging CO groups. Vozdvizhenskii and co-workers (*48, 49*) tried to correlate absorption regions in the infrared spectra of palladium carbonyl halides with the degree of reduction of palladium, and they proposed:

(1) Palladium(II) carbonylhalides have CO stretching frequencies in the range 2100–2200 cm^{-1};

(2) Polymeric carbonyl halides of palladium(I), with compositions close to PdCOX, have CO stretching frequencies in the range of 1850–2000 cm^{-1};

(3) Bridged carbonyls of zero-valent palladium have CO stretching frequencies in the range of 1700–1850 cm^{-1}.

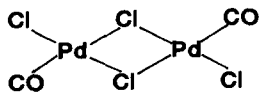

FIG. 9. The structure of $[Pd_2(CO)_2Cl_4]$ proposed by Calderazzo and Dell'Amico (*50*).

The CO frequencies for each oxidation state of Pd are summarized in Table 3.

IR frequencies for CO interacting with copper have been determined in a number of studies (*62, 66*), and they routinely lie in the region of 2050–2120 cm^{-1} for CO associated with Cu(I). Cu(I)–CO and Cu(0)–CO complexes are characterized by substantial stability because of the ability of low valence ions and metal atoms to form π bonds with the CO molecule, and this backbonding makes Cu(I)–CO ligands particularly stable. Cu(II)–CO interactions, however, are very unstable.

Band Assignments

The main factors influencing the CO frequencies in these Pd complexes are: (a) the bonding coordination of the CO group (terminal or bridge); (b) the oxidation state of palladium; and (c) the nature of the other ligands. When CO is coordinated to a Pd cation rather than a zero-valent Pd atom in a cluster, Table 4 indicates that terminal and bridged CO species have their frequency increased by about 100 cm^{-1}. In zero-valent Pd clusters or on metallic Pd surfaces, the bridged-bonded structure typically provides bands that are 200 cm^{-1} or more lower than the linearly bonded structure. Table 3 indi-

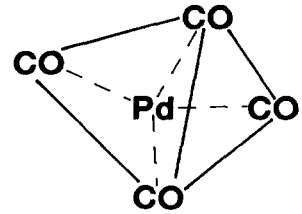

FIG. 10. The structure of $[Pd(CO)_4]$ proposed by Kundig *et al.* (*55*).

TABLE 3

Literature Values of IR Frequencies for CO Coordinated in Pd Chloro-carbonyl Compounds

Oxidation state	Pd complex	ν(CO)(cm^{-1})[a]	Reference
Pd(II)	$Pd(CO)Cl_3^-$	2132_s	(*51*)
		2120_s	(*51*)
		2146_s	(*50*)
		2141_s	(*50*)
	$Pd_2(CO)_2Cl_4$	2159_s–2167_s	(*50*)
Pd(I)	$(PdCOCl)_n$	2003_w, 1972_s, 1942_w	(*45*)
		1975_m, 1925_s, 1892_w	(*46*)
		1978_m, 1940_s	(*47*)
		1985_m, 1978_m, 1945_s, 1940_s	(*48*)
		1977_s	(*37*)
		2023_w, 2002_w, 1978_s, $1951_{w,sh}$, 1936_w	(*44*)
		1960, 1930_s	(*48, 49*)
	$[Pd(CO)CH_3COO]_4$	1975, 1940_s	(*56*)
	$Pd_2(CO)_2Cl_4^{-2}$	1966_m, 1906_s	(*43*)
		1969_m, 1907_s	(*44*)
	$PdCl(CO)_3PhCN$	1979_m, 1954_s, 1948_s	(*44*)
Pd(0)	$Pd(CO)_4$	2060_s	(*55*)
	$Pd_4[P(C_6H_5)_2CH_3]_4(CO)_4$	1840_m, 1820_s	(*57*)
	$Pd_{10}(CO)_{12}[P(n\text{-}C_4H_9)_3]_6$	1890_m, 1853_s, 1800	(*58*)
Pd(0)	Metallic Pd-single crystal surfaces	2120–2050; single-bond	(*53*)
		2000–1800; double-bond	(*53*)
		1880–1800; triple-bond	(*53*)

[a] s—strong, m—medium, w—weak, sh—shoulder.

TABLE 4

The Influence of Pd Oxidation State and the Type of CO Bonding on Carbonyl Wavenumbers

Oxidation state	Form of CO bonding	Example of Pd complex	ν_{CO} (cm^{-1})	Reference
Pd(II)	Terminal	$Pd_2(CO)_2Cl_4$	2120–2170	(*50*)
Pd(I)	Bridged	$[Pd_2(CO)_2Cl_4]^{-2}$	1900–1990	(*43*)
		$[Pd(CO)CH_3COO]_4$	1900–1990	(*56*)
Pd(0)	Terminal	$Pd(CO)_4$	2030–2060	(*55*)
cluster	Bridged	$Pd_4[P(C_6H_5)_2CH_3]_4(CO)_4$	1800–1900	(*57*)
		$Pd_{10}(CO)_{12}[P(n\text{-}C_4H_9)_3]_6$	1800–1900	(*58*)
Pd(0)	Terminal	Metal surf.	2050–2100	(*53*)
	Bridged (Two-fold coord.)	Metal surf.	1880–2000	(*53*)
	Bridged (Three-fold coord.)	Metal surf.	1800–1880	(*53*)

cates that other ligands in the coordination sphere do not markedly alter the bands and give shifts much smaller than either of the first two factors. Thus, CO frequencies between 2100 and 2200 cm^{-1} can be assigned only to terminal CO groups in Pd(II) complexes, bands between 2030 and 2100 cm^{-1} are associated with CO terminally bonded to Pd(0) atoms, CO bands from 1900 to 2000 cm^{-1} represent CO bridge bonded to Pd(I) cations or doubly bonded on metallic Pd crystallites, and bands below 1900 cm^{-1} would most likely imply CO doubly coordinated in zero-valent Pd clusters, although triply bonded CO on metallic Pd is a less likely possibility.

As shown in Figs. 4 and 5, five carbonyl peaks at 1930_s, 1990, 2090, 2100, and 2158 cm^{-1} were identified in the initial 2% Pd/δ-Al_2O_3 catalyst. The peak at 2158 cm^{-1} is quite close to that reported by Calderazzo and Dell'Amico (*50*) for Pd(II) species, which lay between 2159 and 2167 cm^{-1} depending on the solution. From the analysis just mentioned, this 2158-cm^{-1} peak is assigned to a carbonyl group in a Pd(II) compound, most likely $Pd_2(CO)_2Cl_4$. This assignment is supported by the fact that the 2158-cm^{-1} peak grew with increasing oxygen pressure in the $PdCl_2$–$CuCl_2$/δ-Al_2O_3 catalyst at the expense of the 1930-cm^{-1} band (*27*), which is going to be assigned to carbonyl groups coordinated with Pd(I) cations. This behavior indicates that O_2 can oxidize Pd(I) carbonyl complexes to Pd(II) species.

The peaks at 2090 and 2100 cm^{-1} can be straightforwardly associated only with CO terminally adsorbed on palladium metal surfaces, as mentioned previously. The two overlapping peaks may be due to different Pd metal particle sizes with different distributions of low index planes; then the disappearance of the 2100-cm^{-1} band and the retention of the 2090-cm^{-1} band in Figs. 4 and 5 might imply that smaller particles associated with the former have agglomerated or refacetted, thus the latter band is retained. Alternatively, these two peaks may represent linearly adsorbed CO on different faces of very small zero-valent Pd clusters.

The positions of the two peaks at 1930 and 1990 cm^{-1} agree well with bands reported for bridged carbonyls in palladium(I) compounds and for bridge-bonded CO on Pd metal surfaces; consequently, there is some uncertainty regarding unambiguous assignments. However, an examination of the behavior of these two peaks in the presence of H_2O allows a reasonable choice to be made. As shown in Figs. 5b and 5c, the introduction of water vapor to the catalyst markedly decreased the intensity of the 1930-cm^{-1} peak, whereas the 1990-cm^{-1} band changed little. After an IR spectrum was taken under reaction conditions at 303 K, as in Fig. 5d, the CO in the feed was stopped and IR spectra were taken every 2 min to obtain the traces in Fig. 11a. These spectra show the peaks at 2090 and 1990 cm^{-1} change little with time, whereas the 1930-cm^{-1} band loses some intensity. Similar behavior occurs at 323 K, but all the peak intensities decrease noticeably at 343 K, as shown in Fig. 11b. These trends suggest that the 2090- and 1990-cm^{-1} peaks vary in concert in the presence of water and oxygen, and since the 2090-cm^{-1} band has already been assigned to CO adsorbed on palladium metal, the 1990-cm^{-1} band would also be associated with palladium metal. This conclusion is consistent with the greater stability of these two bands (Fig. 11) and the lower activity of metallic Pd for CO oxidation. The significant decrease in the 1930-cm^{-1} peak at only 303 K implies a relatively unstable complex whose concentration is decreased by either decomposition or reaction as the gas-phase CO is swept from the IR cell. These bands on reduced alumina-supported Pd are quite stable over this temperature range, even in the absence of gas-phase CO (*54*).

The only peak left unassigned in this $PdCl_2$/δ-Al_2O_3 catalyst is the one at 1930 cm^{-1}; however, there are three reasons to associate it with bridged carbonyl ligands in Pd(I) complexes. The first is the position of the peak relative to the strong band near

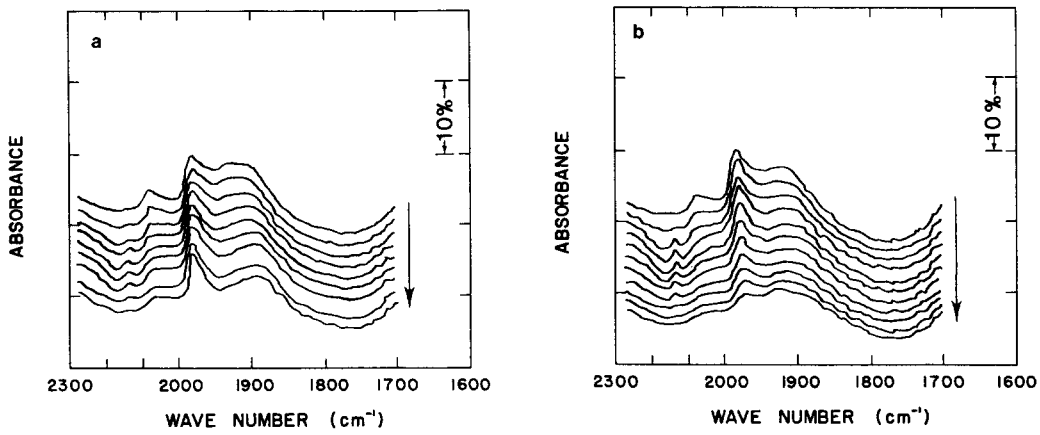

FIG. 11. Transient IR spectra for the 2% Pd/δ-Al_2O_3 after removing CO from the feed. Total pressure = 750 Torr. Each scan required 2 min.
(a) He + 5.3 Torr H_2O + 132 Torr O_2 at 303 K, total time, 20 min;
(b) He + 5.3 Torr H_2O + 132 Torr O_2 at 343 K, total time, 20 min.

1925–1940 cm^{-1} reported for $[PdCOCl]_n$ in various solutions. Second, under reaction conditions with 132 Torr O_2 present, the 1930 cm^{-1} grew with increasing temperature then reversibly decreased back to its original intensity as the temperature was lowered. Colton *et al.* (*37*) have mentioned that Pd metal is not oxidized by dioxygen alone at room temperature; however, as temperature increases oxidation to Pd(I) species would be favored, as indicated by Figs. 5d to 5f. Finally, during the study of the bimetallic catalyst (*27*), it was found that the introduction of water vapor to the system again markedly decreased the 1930-cm^{-1} peak; however, in this case the addition of O_2 allowed the peak to be fully recovered at 303 K. This behavior is shown in Fig. 12, and the facile redox capability of Pd provided by the Cu(I)–Cu(II) couple has been well established in studies of the Wacker process. Although evidence for this assignment of the 1930-cm^{-1} band is very strong, bridge-bonded CO species adsorbed on supported Pd metal particles have been reported with bands in this region, thus a contribution from such species, although unlikely, cannot be completely discounted; however, on metallic Pd these species routinely decrease as temperature increases (*54*) and they do not increase with increasing O_2 pressure (*28*).

The assignment of the CO peak associated with copper is not difficult, and the single peak in Fig. 6 (as well as the 2115-cm^{-1} peak in Fig. 12) is almost undoubtedly that of CO coordinated to Cu(I), i.e., the CuCOCl species. It should also be mentioned that the peak at 1620 cm^{-1} can be assigned to the bending mode of physically adsorbed water molecules or –OH groups on the alumina surface. This assignment is consistent with the increase in intensity when H_2O vapor is introduced and the decrease in intensity as the temperature is raised. A single reference wafer of pure Al_2O_3 was used for all runs and was subjected to a variety of treatments, thus perfect cancellation of adsorbed H_2O and –OH groups on the alumina was not attained, and thus a rather broad band near 1620 cm^{-1} can frequently be observed in the IR spectra.

Kinetic Behavior

The oxidation of CO using noble metal complexes in solution as a catalyst has been extensively investigated, and studies of this homogeneously catalyzed reaction have

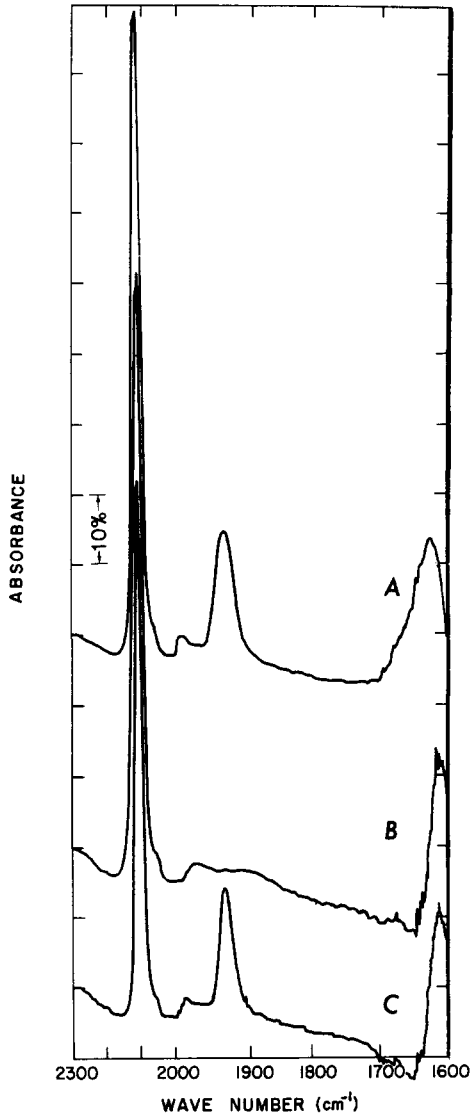

FIG. 12. IR spectra for 1.8% Pd–11.9% Cu/δ-Al_2O_3 with and without water vapor in the presence of CO. Gas flow = 28.5 cm^3/min, total pressure = 750 Torr.
(a) He + 26 Torr CO at 303 K;
(b) He + 26 Torr CO at 5.3 Torr H_2O at 303 K;
(c) He + 26 Torr CO at 5.3 Torr H_2O + 132 Torr O_2 at 303 K.

been reviewed by Eisenberg and Hendriksen (*67*). As they point out, CO may act as a reductant and form CO_2 in three different ways:

(1) As a direct oxygen acceptor;

(2) As a two-electron reductant with H_2O as the oxygen source;

(3) As an indirect reductant to make hydrogen via the water gas shift reaction which then carries out the observed reduction. However, this review mentions nothing about CO oxidation in systems containing $CuCl_2$ or $PdCl_2$. No investigations have been found involving this reaction over $CuCl_2$-only catalysts, and only one kinetic study of CO oxidation by dioxygen using $PdCl_2$ catalysts has been reported (*24*).

Golodov *et al.*(*21*) observed that reaction rates in aqueous phases of $PdCl_2$ and $CuCl_2$ are higher with oxygen than without oxygen. They have proposed a mechanism involving either rapid CO insertion into a Pd–dioxygen complex along the *trans* coordinate (steps (2) and (3)) or dioxygen displacement from the Pd(II) coordination sphere by CO (steps (4) and (5)). These steps are

$$[PdCl_4]^{-2} + O_2 \rightleftharpoons [PdCl_3O_2]^- + Cl^- \quad (1)$$

$$[PdCl_3O_2]^- + CO \rightleftharpoons [O_2PdCl_2CO] + Cl^- \quad (2)$$

$$[O_2PdCl_2CO] + H_2O \rightarrow Pd(0) + CO_2 + 2HCl + O_2 \quad (3)$$

or

$$[PdCl_4]^{-2} + O_2 \rightleftharpoons [PdCl_3O_2]^- + Cl^- \quad (1)$$

$$[PdCl_3O_2]^- + CO \rightleftharpoons [PdCl_3CO]^- + O_2 \quad (4)$$

$$[PdCl_3CO]^- + H_2O \rightarrow Pd(0) + CO_2 + 3Cl^- + 2H^+ \quad (5)$$

Kinetically, the reaction order for CO is unity in either sequence.

Zhizhina *et al.*(*22, 23*) have also studied CO oxidation in aqueous solutions of $PdCl_2$ and other compounds; however, they concluded that Pd(I) carbonyl complexes were the active species in this reaction, and their proposed reaction mechanism is the sequence

$$Pd(II) + CO + H_2O \xrightarrow{slow} Pd(0) + CO_2 + 2H^+ \quad (6)$$

$$Pd(0) + Pd(II) + CO \rightleftharpoons Pd_2(I)(CO) \quad (7)$$

$$Pd_2(I)(CO) + Ox. \xrightarrow{fast} Pd(II) + Pd(0) + CO_2 + Red. \quad (8)$$

$$Pd(0) + Ox. \rightarrow Pd(II) + Red. \quad (9)$$

where Ox. is an oxidizing agent and Red. is the reduced oxidant.

In their study of CO oxidation over $PdCl_2$ on charcoal in a hydrogen chloride solution, Fujimoto *et al.* reported negative activation energies, positive reaction orders for CO and H_2O, and a zero-order dependence on O_2 (*24*). Assuming chemistry analogous to ethylene oxidation in the Wacker process (*68*), they proposed a complicated reaction mechanism which contained a step for decomposition of Pd carbonyls; however, a quantitative fit of the derived rate equation to the kinetic data was not determined in this paper (*24*).

Reaction Mechanism over $PdCl_2$ Catalysts without Water Vapor in the Feed

As mentioned earlier in the Experimental section, the 2% Pd/δ-Al_2O_3 catalyst was prepared from $PdCl_2$; therefore, Pd(II) is initially expected instead of Pd(I). Fleisch *et al.* (*69*) prepared a 2% Pd/SiO_2 catalyst using $PdCl_2$ and a preparation procedure similar to that used here, and they found with UV-spectroscopy that only Pd(II) compounds existed initially, with $(PdCl_4)^{-2}$ and $PdCl_2(H_2O)_2$ being the major Pd complexes. However, in the present work the major peaks observed with CO present were assigned to Pd(I) and Pd(0); therefore, $PdCl_2$ in the presence of CO and adsorbed H_2O is mostly reduced to Pd(I) or Pd(0) carbonyl-containing complexes, with the former initially predominating at 303 K. Such a reduction procedure is not unusual and could be expected from previous studies which have shown that Pd(II) can be easily reduced to palladium metal by CO and H_2O, probably via Pd(I) compounds (*37*). Adsorbed water and hydroxyl groups exist on the support surface, as demonstrated by the IR spectra; consequently, three of the first reactions with CO are proposed to be Eqs. (10), (11), and (12) in the overall sequence which is proposed on the next page. These reactions produce the species observed in Figs. 4 and 5. Increasing the CO pressure from 0.4 to 26 Torr increases the Pd(I) carbonyl band at 1930 cm^{-1} and suppresses the Pd(II) carbonyl species at 2158 cm^{-1}, but produces no significant change in the amount of CO on metallic Pd, as shown in Figs. 4b and 4c. This reduction by CO was very fast because the peak for Pd(I) carbonyls grew rapidly as CO was fed into the IR cell.

Cotton and Wilkinson (*70*) mention that molecular oxygen can be reduced to either O_2^{-1} or O_2^{-2} without the O–O bond being broken, and each of these species can act as a ligand toward transition metals. Consequently, the interaction of O_2 with PdCl to form a $PdClO_2$ complex might be anticipated. In fact, this precise reaction has been shown to occur with $PdCl_2$/δ-Al_2O_3 catalysts at 340 K (and lower) (*71*). Sass *et al.* used ESR to monitor the concentration of the O_2^- radical during formation of the $[Pd(II)ClO_2]^-$ species and, in addition, they demonstrated its reactivity with CO in the absence of water (*71*). It is proposed here that the O_2 bond rupture to form the CO–O bond is the rate determining step (rds) and that it occurs in a Pd dimer complex as shown below.

$$PdCl_2 + CO + H_2O_{ad} \overset{K}{\rightleftharpoons} Pd(0) + CO_2 + 2HCl_{ad} \quad (10)$$

$$2PdCl_2 + CO + H_2O_{ad} \overset{K_1}{\rightleftharpoons} 2PdCl + CO_2 + 2HCl_{ad} \quad (11)$$

$$PdCl + CO \overset{K_{CO}}{\rightleftharpoons} PdClCO \quad (12)$$

$$PdCl + O_2 \overset{K_{O_2}}{\rightleftharpoons} PdClO_2 \quad (13)$$

$$PdClCO + PdClO_2 \overset{K_2}{\rightleftharpoons} \underset{I}{Pd_2Cl_2(CO)O_2} \quad (14)$$

$$\underset{\text{I}}{Pd_2Cl_2(CO)O_2} \xrightarrow{k_3,\text{rds}} PdCl + CO_2 + \underset{\text{II}}{OPdCl} \quad (15)$$

$$\underset{\text{II}}{OPdCl} + CO \overset{K_4}{\rightleftharpoons} PdCl + CO_2 \quad (16)$$

This sequence of steps involves only the water initially present from the impregnation step in the first reaction. The first four reactions occur readily and are assumed to be in quasi-equilibrium. The decrease in the 1930-cm^{-1} peak intensity can be attributed to a decrease in the PdCl concentration due to its interaction with O_2, thus shifting reaction (12) to the left.

This is the mechanism associated with the *initial* low temperature reactivity in the absence of water vapor in the feed. The rapid formation of the 1930-cm^{-1} peak assigned to PdCOCl, the concomitant evolution of CO_2 measured by gas chromatography, and the increase in the 1930-cm^{-1} peaks as CO pressure increases are all consistent with these equilibrated steps preceding the slow step (15). The rate equation derived from this model is discussed later.

The structure of intermediate (I) is not known, but one possibility, illustrated in Fig. 13, can be proposed based on studies of cobalt species interacting with O_2 (*72, 73*). By analogy, the structure of (I) in Fig. 13a would be formed representing an O_2^{-1} bridge

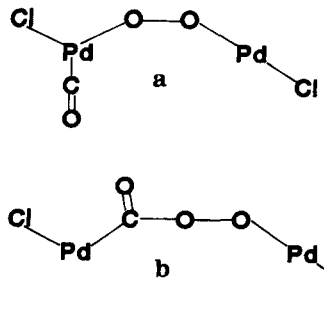

FIG. 13. Possible structures of intermediate [I] in Eq. (15).

with Pd in a +2 state and it would pass through the configuration in Fig. 13b as it decomposed. Intermediate (II) in Eq. (15) would be quite reactive. It must be remembered that the PdClCO species in step (14) is a stoichiometric representation of the monomer that exists in a more complicated chain structure due to the bridge-bonding behavior of CO as shown in Fig. 7.

Reaction Mechanism over $PdCl_2$ Catalysts with Water Vapor in the Feed

The sequence of steps proposed for CO oxidation in the presence of H_2O vapor is similar to the chemistry proposed previously, yet there are notable differences to explain the marked rate enhancement that is observed. The first is the establishment of a thin layer of water (probably a monolayer) on the alumina surface thus providing a two-dimensional, high surface area water phase analogous to a homogeneous aqueous phase. Second, the rapid reduction of Pd(II) species in water by CO is well established (*21, 37, 74*), and this reaction can now occur in this adsorbed water phase. Finally, the rate determining step now shifts to the reoxidation of Pd(0) by dioxygen because of the rapidity of interaction between water and the Pd–chlorocarbonyl species. This provides the first-order dependency on O_2 observed experimentally. The large activity increase in the presence of low concentrations of H_2O can be attributed to a larger solubilized fraction of the $PdCl_2$ precursor in addition to the high reactivity of molecular water with $[PdClCO]_n$ species to give CO_2 and hydrogen, a reaction which is similar to the water gas shift reaction. Although the reaction between PdClCO and $PdClO_2$ can still occur, its contribution to the overall rate is inconsequential. The proposed mechanism describing CO oxidation in the presence of water vapor is

$$H_2O_{(g)} \overset{K_{H_2O}}{\rightleftharpoons} H_2O_{(ad)} \quad (17)$$

$$PdCl_2 + H_2O_{(ad)} \overset{K_1}{\rightleftharpoons} PdCl_{2(aq)} \quad (18)$$

$$2PdCl_{2(aq)} + CO + H_2O_{(ad)} \overset{K_2}{\rightleftharpoons} 2PdCl_{(aq)} + CO_2 + 2HCl_{(ad)} \quad (19)$$

$$PdCl_{(aq)} + CO \overset{K_{CO}}{\rightleftharpoons} PdClCO_{(aq)} \quad (20)$$

$$PdCl_{(aq)} + O_2 \overset{K_{O_2}}{\rightleftharpoons} PdClO_{2(aq)} \quad (21)$$

$$PdClCO_{(aq)} + H_2O_{(ad)} \overset{K_3}{\rightleftharpoons} Pd(0) + CO_2 + HCl_{(aq)} + \tfrac{1}{2}H_{2(aq)} \quad (22)$$

$$Pd(0) + PdClO_2 + HCl_{(aq)} \overset{K_4}{\rightleftharpoons} \underset{III}{HPd_2Cl_2O_2} \quad (23)$$

$$\underset{III}{HPd_2Cl_2O_2} \xrightarrow{k_5,\text{rds}} 2PdCl + HO_{2(aq)} \quad (24)$$

$$HO_{2(aq)} + 3Pd(0) + 3HCl \overset{K_6}{\rightleftharpoons} 3PdCl + 2H_2O \quad (25a)$$

or

$$HO_{2(aq)} + 3H_{(ad)} \overset{K_7}{\rightleftharpoons} 2H_2O \quad (25b)$$

The first three steps establish the active Pd(I) species and the catalytic cycle consists of steps (20) to (25). It has been stated previously that reoxidation of Pd(0) in dioxygen can be difficult, and it is suggested here that PdCl facilitates this reaction by activating O_2 via the $PdClO_2$ species. Although the details of the reoxidation of Pd(0) to Pd(I) are not known, a peroxide intermediate may exist in step (25) as proposed by Cotton and Wilkinson (*70*).

The IR results are consistent with this model as Fig. 5b shows the sharp decrease in the 1930-cm^{-1} peak upon addition of H_2O, and the evolution of CO_2 during this period, detected by gas chromatography, supports the reaction shown in step (22). The presence of some metallic palladium is indicated by the bands at 2090 and 1990 cm^{-1} although they did not grow when water was added; instead, the broad band between 1900 and 2000 cm^{-1} appeared to strengthen, especially at higher temperature (353–363 K). If the equilibrium of step (22) lies far to the right, the IR peaks for $[PdClCO]_n$ are expected to be weak.

Although the $PdCl_2$/carbon catalyst gave partial pressure dependencies on CO and O_2 that were noticeably different from the $PdCl_2/\delta$-Al_2O_3 catalyst, the model can still explain them. The activation energy of 4.7 kcal/mol for $PdCl_2$/C, compared to 9.2 kcal/mole for $PdCl_2/\delta$-Al_2O_3, is suggestive of diffusion control, which is a possibility with this high surface area carbon black. However, the specific activities of the two catalysts are similar, and application of the Weisz criterion indicated that diffusional limitations are minimal for both catalysts (*75*). Furthermore, Fujimoto *et al.* (*24*) actually reported a negative activation energy for their $PdCl_2$/carbon catalyst; thus the situation is complicated. Regardless, the low and sometimes negative apparent energies for these C-supported catalysts are almost certainly due to the adsorption behavior of H_2O on carbon as a function of temperature. The lower coverages at higher temperature would tend to decrease activity according to our model.

These two mechanisms in the presence and absence of vapor phase water are consistent with our IR and kinetic results as well as recent results in the literature but, although no new species are proposed, the mechanisms are significantly different from those proposed previously (*21, 24*). There are several reasons for this. First, the negative dependence on CO and strong positive dependence on O_2 found for the $PdCl_2/\delta$-Al_2O_3 catalyst had to be explained. These dependencies differ from those reported by Fujimoto *et al.* (*24*) and cannot be obtained by assuming a mechanism analogous to that for C_2H_4 oxidation in the Wacker process. Second, the *in situ* IR characterization, which had surprisingly not been reported before, provided additional information which had to be accommodated by the mechanism. Finally, recent work in the literature, such as the identification of the Pd ClO_2 species by ESR and the establishment

of its activity with CO (*71*), justifies some of the proposed steps.

Reaction Mechanism over $CuCl_2$ Catalysts without Water Vapor in the Feed

Golodov and co-workers have shown that CO reduces $CuCl_2$ in aqueous solution in a manner analogous to that for $PdCl_2$ (*74, 76*). Therefore, reduction to Cu(I) is expected, and the IR band at 2115 cm^{-1} in Fig. 6 is confirmation that Cu(I) species are formed. The remainder of the sequence is assumed to be identical to that for $PdCl_2/\delta\text{-}Al_2O_3$ in the absence of water vapor, i.e., steps (11) through (16) are repeated with $CuCl_2$ and they involve Cu(I) and Cu(II) oxidation states.

Derivation of Reaction Rate Expressions

Kuznetsova *et al.* (*77*) have stated that only water-soluble agents are active in CO oxidation. Although this may not be absolutely correct, it does indicate the strong positive effect of molecular water on these Pd and Cu complexes. Consequently, it is assumed that an adsorbed water layer is needed to dissolve and activate these complexes. After impregnation, the $\delta\text{-}Al_2O_3$ catalyst contains about 5% water by weight, which is approximately one monolayer in this larger-pore alumina. For the carbon support, the water content was over 60 wt%, which represents about 1.5 monolayers of H_2O and indicates capillary condensation may be occurring in the smallest pores. Thus with both supports, there is some water present on the surface for partial activation of the dispersed metal salts.

Rate expressions are derived from the sequences of steps previously described based upon the following set of assumptions:

(1) The most abundant Pd species are PdCl, PdClCO, and $PdClO_2$;

(2) The most abundant Cu species are CuCl, CuClCO, and $CuClO_2$;

(3) The chloride ion is in excess and is considered to be constant;

(4) When water vapor is present, water can form thin films or islands on the surface of the support which provide a two-dimensional analogue of very active Pd or Cu complexes in homogeneous aqueous systems;

(5) The Pd or Cu complexes in this thin film are readily accessible to CO and O_2; thus they can be considered as adsorption sites analogous to those on a solid surface.

For example, with Pd a site balance can then be made, i.e.,

$$L = [PdCl] + [PdClCO] + [PdClO_2] \quad (26)$$

where L is the total number of these complexes.
The fractions interacting with a CO or O_2 molecule can be shown to be

$$\theta_{CO} = \frac{K_{CO}P_{CO}}{1 + K_{CO}P_{CO} + K_{O_2}P_{O_2}} \quad (27)$$

and

$$\theta_{O_2} = \frac{K_{O_2}P_{O_2}}{1 + K_{CO}P_{CO} + K_{O_2}P_{O_2}} \quad (28)$$

which are analogous to a Langmuir isotherm.

For the Pd catalysts without water vapor, using the stated assumptions, the rds (step (15), the series of quasi-equilibrated steps, and Eqs. (27) and (28), the rate expression below can be derived (*75*).

$$r = Lk_3K_2\frac{K_{CO}K_{O_2}P_{CO}P_{O_2}}{(1 + K_{CO}P_{CO} + K_{O_2}P_{O_2})^2} = \frac{kK_{CO}K_{O_2}P_{CO}P_{O_2}}{(1 + K_{CO}P_{CO} + K_{O_2}P_{O_2})^2} \quad (29)$$

For the Pd catalysts with water vapor present, the concentration of very active solubilized Pd complexes, that is, the number of active sites, will be proportional to the coverage of the H_2O film, as stated in assumption 4. If water adsorption on the support is described by a Langmiur isotherm, i.e.,

$$[H_2O_{ad}] = \frac{K_{H_2O}P_{H_2O}}{1 + K_{H_2O}P_{H_2O}}, \quad (30)$$

then the form of the reaction rate expression is:

$$r = \left(\frac{LK_5K_4K_3}{[CO_2][H_2]^{1/2}}\right)\left(\frac{K_{CO}K_{O_2}P_{CO}P_{O_2}}{(1 + K_{CO}P_{CO} + K_{O_2}P_{O_2})^2}\right)\left(\frac{K_{H_2O}P_{H_2O}}{1 + K_{H_2O}P_{H_2O}}\right) \quad (31)$$

and, if $L \propto [H_2O_{ad}]$ and the amounts of CO_2 and H_2 are assumed to be approximately constant in the catalyst bed under steady-state reaction conditions, then the final expression is

$$r = k\left(\frac{K_{CO}K_{O_2}P_{CO}P_{O_2}}{(1 + K_{CO}P_{CO} + K_{O_2}P_{O_2})^2}\right)\left(\frac{K_{H_2O}P_{H_2O}}{1 + K_{H_2O}P_{H_2O}}\right)^2 \quad (32)$$

An identical expression is of course derived for the $CuCl_2$ catalysts (*75*).

Using the direct search simplex method for optimization, the constants k, K_{CO}, K_{O_2} and K_{H_2O} in Eqs. (29) and (32) were computed for both $PdCl_2$ and $CuCl_2$ catalysts by fitting these equations to the partial pressure data. These results are given in Table 5 and they are compared with the data in Fig. 3. The models describe both the palladium and copper catalysts relatively well. It is not easy to compare the constants directly because the reaction temperature varies significantly; however, some evaluation of the physical consistency of these fitted parameters can be made. First, the apparent rate constant, which is a complicated multiple of parameters, does increase markedly upon the addition of water vapor, as observed, and also increases with temperature. Second, the values of K_{CO} for 2% Pd/δ-Al_2O_3 (without H_2O, IR) and 12% Cu/δ-Al_2O_3 (without H_2O, IR) can be compared. There was much greater IR peak intensity for the [PdCOCl] species in the 2% Pd/δ-Al_2O_3 catalyst compared to CuCOCl in the 12% Cu/δ-Al_2O_3 catalyst, as indicated in Figs. 5b and 6a. The value of K_{CO} for the 2% Pd/δ-Al_2O_3 catalyst is indeed much larger than that for the 12% Cu/δ-Al_2O_3 catalyst. Third, with the 2% Pd/δ-Al_2O_3 catalyst in the presence of

TABLE 5

Computed Constants (k, K_{CO}, K_{O_2}, K_{H_2O}) for Unreduced Pd and Cu Catalysts

Catalyst	Reaction temp. (K)	Constants			
		k	K_{CO}	K_{O_2}	K_{H_2O}
2% Pd/δ-Al_2O_3 (without H_2O, IR)	403	0.74	3.1×10^5	8.0×10^3	
2% Pd/δ-Al_2O_3 (with H_2O, IR)	323	4.8	2.6×10^3	2.7×10^1	3.0×10^2
12% Cu/δ-Al_2O_3 (without H_2O, IR)	423	0.86	5.4×10^1	1.2×10^1	
2% Pd/carbon (with H_2O, reactor)	353	0.73	3.7×10^3	2.3×10^2	2.1×10^2
12% Cu/carbon (with H_2O, reactor)	433	0.77	7.3×10^1	2.0×10^1	8.6×10^3
2% Pd/δ-Al_2O_3 (with H_2O, reactor)	343	0.14	2.8×10^4	7.8×10^2	
	363	0.25	3.0×10^3	1.6×10^2	
	383	0.49	2.7×10^2	4.4×10^1	
	383[a]	0.68	3.6×10^3	5.4×10^1	

[a] After oxygen treatment at 363 K for 5 h.

water vapor (reactor study), the apparent reaction rate constant increases and the equilibrium "adsorption" constants decrease with ascending temperature. The computed activation energy for this 2% Pd/δ-Al_2O_3 catalyst is 8.3 kcal/mole, which is close to the experimental value of 9.2 kcal/mole.

The computed enthalpy for CO interacting with $PdCl_{(aq)}$, ΔH_{CO}, is -30.3 kcal/mole, which is higher than the literature value of -13.6 kcal/mole determined by Dell'Amico *et al.* (*78*) for PdClCO in methyl dichloride, but in the absence of water. However, the computed enthalpy for the O_2 interaction, $\Delta H_{O_2} = -19.6$ kcal/mole, is close to a literature value of -18.1 kcal/mole (*79*). Deactivation was observed at 363 and 383 K with this catalyst, but an O_2 treatment at 363 K for 5 h markedly enhanced the activity, as shown in Figs. 3g and 3h, and the catalyst recovered its original activity. From Table 5, the computed k and K_{O_2} values at 383 K did not change much after the O_2 treatment; however, the K_{CO} value at 383 K was enhanced by an order of magnitude after O_2 treatment. Therefore, k and K_{O_2} values depend little on the oxygen treatment. Because of deactivation, K_{CO} values are noticeably reduced, which makes the computed ΔH_{CO} larger than expected. If ΔH_{CO} is computed between the data points at 343 and 383 K after the O_2 treatment, the ΔH_{CO} value becomes -6.7 kcal/mole, which is closer to the reported value mentioned above.

SUMMARY

Rates of CO oxidation over unreduced Pd or Cu catalysts are lower compared to those in the bimetallic catalysts. With water vapor present in the feed, the activity is greatly enhanced over unreduced $PdCl_2$ catalysts and the activation energy is reduced. Therefore, water gives a positive effect on the activity of unreduced Pd catalysts, but it has a negative effect on unreduced Cu catalysts. The role of water in CO oxidation over unreduced Pd catalysts is not absolutely clear, but one principal function appears to be the activation of PdClCO species by solubilizing $PdCl_2$. The trends of partial pressure dependency on CO and O_2 over unreduced Pd and Cu catalysts are the same as those reported for reduced Pd and Cu metal catalysts, which means a negative dependency on CO over the Pd catalyst, and a positive dependency on CO over the Cu catalysts and a positive dependency on O_2 over both catalysts. The Pd(II) precursor is reduced by CO to give Pd(I) carbonyls, which react rapidly with water vapor to form CO_2 and Pd metal. On these supported catalysts, this Pd metal is catalytically oxidized back to Pd(I) by dioxygen.

IR peaks at 2090 and 1990 cm^{-1} are associated with terminal and bridged CO species, respectively, adsorbed on metallic Pd particles, and this assignment is supported by the fact that both peaks changed similarly and simultaneously. A peak at 2158 cm^{-1} is related to the terminal carbonyl in the Pd(II) compound ($PdCl_2CO$), and a peak at 1930 cm^{-1} is assigned to the carbonyl in the Pd(I) compound $(PdClCO)_n$. However, the 1930-cm^{-1} peak also can be associated with triply coordinated carbonyls on Pd metal and, although it is very unlikely, a contribution from such species cannot be completely discounted. In the Cu catalyst, the only observed peak at 2115 cm^{-1} is almost undoubtedly that of CO coordinated to Cu(I); i.e., (CuClCO).

A rather complex series of steps is required to explain both the IR and the kinetic behaviors. However, the proposed steps have precedent in the literature and provide plausible reaction sequences that produce derived rate expressions consistent with experimental results. Water appears to play a very important role both as a two-dimensional solvent for the $PdCl_2$ and $CuCl_2$ compounds and as a reactant with Pd complexes to produce CO_2. In the absence of water vapor in the feed, CO_2 is produced directly from O_2.

ACKNOWLEDGMENTS

This research was sponsored by a grant from Teledyne Water Pik, Fort Collins, CO. Helpful discussions with Professor A. Sen, Chemistry Department, The Pennsylvania State University, are also acknowledged.

REFERENCES

1. Collins, M. F., *in* "Ventilation '85" (H. D. Goodfellow, Ed.), Elsevier, Amsterdam, 1986.
2. Brittain, M. I., *AIChE J.* **16,** 305 (1970).
3. Langmuir, I., *Trans. Faraday Soc.* **17,** 672 (1922).
4. Baddour, R. F., Modell, M., and Goldsmith, R. L., *J. Phys. Chem.* **74,** 1787 (1970).
5. Matsushima, T., and White, J. M., *J. Catal.* **40,** 334 (1975).
6. Conrad, H., Ertl, G., and Kuppers, J., *Surf. Sci.* **76,** 323 (1978).
7. Engel, T., and Ertl, G., *J. Chem. Phys.* **69,** 1267 (1978).
8. Engel, T. and Ertl, G., *Chem. Phys. Lett.* **54,** 95 (1978).
9. Cant, N. W., Hicks, P. C., and Lennon, B. S., *J. Catal.* **54,** 372 (1978).
10. Poppa, H., and Soria, F., *Surf. Sci.* **115,** L105 (1982).
11. Stuve, E. M., Madix, R. J., and Brundle, C. R. **146,** 155 (1984).
12. Barshad, Y., and Gilari, E., *J. Catal.* **94,** 468 (1985).
13. Barshad, Y., McCarthy, E., Zahradnik, J., Kuczynski, G. C., and Carberry, J. J., *J. Catal.* **39,** 29 (1975).
14. Vorontsov, A. V., Kasatkina, L. A., Dzisyak, A. P., and Tikhonova, S. V., *Kinet. Katal.* **20,** 1194 (1979).
15. Vorontsov, A. V., and Kasatkina, L. A., *Kinet. Katal.* **21,** 1494 (1980).
16. Liao, P. C., Carberry, J. J., Fleish, T. H., and Wolf, E. E., *J. Catal.* **74,** 307 (1982).
17. Lloyd, W. G., and Rowe, D. R., U.S. Patent #3790662, Feb. 5, 1974.
18. Lloyd, W. G., and Rowe, D. R., Canadian Patent #1011531, Jan. 7, 1977.
19. Desai, M. N., Butt, J. B., and Dranoff, J. S., *J. Catal.* **79,** 95 (1983).
20. Desai, M. N., Ph.D. thesis, Northwestern University, 1980.
21. Golodov, V. A., Kuksenko, E. L., and Sokol'skii, D. V., *Dokl. Akad. Nauk.* **272,** 628 (1983).
22. Zhizhina, E. G., Kuznetsova, L. I., and Matveev, K. I., *React. Kinet. Catal. Lett.* **31,** 113 (1986).
23. Zhizhina, E. G., Matveev, K. I., and Kuznetsova, L. I., *Kinet. Katal.* **26,** 461 (1985).
24. Fujimoto, K., Iuchi, K., and Kunugi, T., *Int. Chem. Eng.* **12,** 741 (1972).
25. Kuznetsova, L. I., Matseev, K. I., and Zhizhina, E. G., *Kinet. Katal.* **26,** 1029 (1985).
26. Edwards, J. F., and Schrader, G. L., *J. Phys. Chem.* **88,** 5620 (1984).
27. Choi, K. I., and Vannice, M. A., *J. Catal.* **127,** 489 (1991).
28. Choi, K. I., and Vannice, M. A., submitted for publication.
29. Palmer, M. B., and Vannice, M. A., *J. Chem. Technol. Biotechnol.* **30,** 205 (1986).
30. Bozon-Verduraz, F., Tardy, M., Bugli, G., Pannetier, G., "Preparation of Catalysts," Vol. 1, p. 256. Elsevier, Amsterdam/New York, 1976.
31. (a) Buitiaux, J. P., Cosyns, J., and Vasudevan, S., p. 123; (b) Gubitosa, G., Berton, A., Camia, M., and Pernicone, N., p. 431; (c) Margitfalvi, J., Szabo, S., Nagy, F., Gobolos, S., and Hegedus, M., p. 473; "Preparation of Catalysts," Vol. 3. Elsevier, Amsterdam/New York, 1983.
32. Vannice, M. A., Moon, S. H., Twu, C. C., and Wang, S.-Y., *J. Phys. E.* **12,** 849 (1979).
33. McCarthy, E., Zahradnik, J., Kuczynski, G., and Carberry, J. J., *J. Catal.* **39,** 29 (1975).
34. Brongersma, H. H., Sparmaay, M. J., and Buck, T. M., *Surf. Sci.* **72,** 657 (1978).
35. Prado-Burguete, C., Linares-Solano, A., Rodriguez-Reinoso, F., and Salinas-Martinez de Lecea, "XVIIth Conf. on Carbon," 82 1987.
36. Stern, E.W., *Catal. Rev.* **1,** 73 (1967).
37. Colton, R., Farthing, R. H., and McCormick, M. J., *Aust. J. Chem.* **26,** 2607 (1973).
38. Manchot, W., and Konig, *J. Chem. Ber.* **59,** 883 (1926).
39. Irving, R. J., and Magnusson, E. A., *J. Chem. Soc.,* 2283 (1958).
40. Sanger, A. R., Schallig, L. R., and Tan, K. G., *Inorg. Chim. Acta* **35,** L325 (1979).
41. Andronov, E. A., Nukushkin, Yu. N., Churakov, V. G., and Murashkin, Yu. V., *Russ. J. Inorg. Chem.* **20,** 634 (1975).
42. Spitsyn, V. I., Fedoseev, I. V., and Znamenski, I. V., *Russ. J. Inorg. Chem.* **25,** 1518 (1980).
43. Goggin, P. L., Goodfellow, R. J., Herbert, I. R., and Orpen, A. G., *J.C.S. Chem. Comm.,* 1077 (1981).
44. Goggin, P. L., and Mink, J., *J.C.S. Dalton Trans.,* 534 (1974).
45. Dent, W. T., Long, R., and Whitfield, G. H., *J. Chem. Soc.,* 1588 (1964).
46. Treiber, A., *Tetrahedron Lett.* 2831 (1966).
47. Schnabel, W., and Kober, E., *J. Organomet, Chem.* **19,** 45 (1969).
48. Kushnikov, Yu. A., Beilina, A. Z., and Vozdvizhenskii, V. F., *Russ. J. Inorg. Chem.* **16,** 218 (1971).
49. Beilina, A. Z., Kushnikov, Yu. A., and Vozdvizhenskii, V. F., *Russ. J. Phys. Chem.* **45,** 594 (1971).
50. Calderazzo, F. and Dell'Amico, D. B., *Inorg. Chem.* **20,** 1310 (1981).

51. Browing, J., Goggin, P. L., Goodfellow, R. J., Norton, M. G., Rattray, J. M., Taylor, B. F., and Mink, J., *J. Chem. Soc. Dalton Trans.*, 2061 (1977).
52. Sheppard, N., and Nguyen, T. T., *Adv. Infrared Raman Spectrosc.* **5,** 67 (1978).
53. Bradshaw, A. M., and Hoffman, F., *Surf. Sci.* **72,** 513 (1978).
54. Vannice, M. A., Wang, S.-Y., and Moon, S. H., *J. Catal.* **71,** 152 (1981).
55. Kundig, E. P., Moskovitz, M., and Ozin, G. A., *Canad. J. Chem.* **235,** 98 (1972).
56. Kuzmina, L. G., and Struchkov, Y. T., *Koord. Khim.* **5,** 1558 (1979).
57. Dubrawski, J., Kriege-Simondsen, J. C., and Feltham, R. D., *J. Amer. Chem. Soc.* **102,** 2089 (1980).
58. Mednikov, E. G., Eremenko, N. K., Mikhailov, V. A., Gubin, S. P., Slovokhotov, Y. L., and Struchkov, Y. T., *J.C.S. Chem. Commun.*, 989 (1981).
59. Vargaftik, M. N., Stromnova, T. A., Khodashova, T. S., Porai-Koshits, M. A., and Moiseev, I. I., *Izv. Akad. Nauk. SSSR Ser. Khim.*, 1690 (1980).
60. Colton, R., McCormick, M. J., and Pannan, C. D., *J.C.S. Chem. Commun.*, 823 (1977).
61. Vargaftik, M.N., Stromnova, T. A., and Moiseev, I. I., *Russ. J. Inorg. Chem.* **25,** 127 (1980).
62. Naccache, C., Primet, M., and Mathieu, M. V., *Adv. Chem. Ser.* **121,** 266 (1973).
63. Busca, G., *J. Mol. Catal.* **43,** 225 (1987).
64. Amara, M., Bettahar, M., Gengenbre, L., and Olivier, D., *Appl. Catal.* **35,** 153 (1987).
65. Rucci, G., Zanzoterra, C., Lachi, M. P., and Camia, M., *J.C.S. Chem. Commun.*, 652 (1971).
66. Whyman, R., *J.C.S. Dalton Trans*, 2294 (1972).
67. Eisenberg, R., and Hendriksen, D. E., *in* "Advances in Catalysis" (D. D. Eley, H. Pines, and P. B. Weisz, Eds.), Vol. 28, p. 79. Academic Press, New York, 1979.
68. Gates, B. C., Katzer, J. R., and Schuit, G. C. A., "Chemistry of Catalytic Processes," McGraw–Hill, New York, 1979.
69. Fleisch, T. H., Hicks, R. F., and Bell, A. T., *J. Catal.* **87,** 398 (1984).
70. Cotton, F. A., and Wilkinson, G., "Advanced Inorganic Chemistry," 4th p. 152. Wiley, New York, 1980.
71. Sass, A. S., Shvets, V. A., Savel'eva, G. A., Popova, N. M., and Kazanski, V. B., *Kinet. Katal.* **27,** 894 (1985).
72. Fronczek, F., Schaefer, W. P., and Marsh, R. E., *Acta Crystallogr.* **B30,** 117 (1974).
73. Vannerberg, N. G., and Brosset, G., *Acta Crystallogr.* **16,** 247 (1963).
74. Golodov, V. A., Shedudyakov, Yu.L., Di, R. I., and Fokanov, V. K., *Kinet. Katal.* **18,** 234 (1977).
75. Choi, K. I., PhD thesis, The Pennsylvania State University, 1990.
76. Shedudyakov, Yu.L., and Golodov, V. A., *J. Mol. Catal.* **7,** 383 (1980).
77. Kuznetsova, L. I., Zhizhina, E. G., and Matveev, K. I., "Homogeneous and Heterogeneous catalysts," VNU, p. 259. Science Press, 1986.
78. Dell'Amico, D. B., Calderazzo, F., and Zandona, N., *Inorg. Chem.* **23,** 137 (1984).
79. Valitov, N. Kh., Ibragimov, F. Kh., and Lysikov, V. M., *Kinet. Katal.* **19,** 103 (1978).